

## Supporting Information for

### NMR Chemical Exchange as a Probe for Ligand-Binding Kinetics in a Theophylline-Binding RNA Aptamer

Michael P. Latham, Grant R. Zimmermann and Arthur Pardi

*Department of Chemistry and Biochemistry, 215 UCB, University of Colorado, Boulder, CO  
80309-0215. USA*

#### **Materials and Methods**

##### ***1D <sup>1</sup>H Experiments***

1D <sup>1</sup>H spectra were collected using a gradient 11-echo pulse sequence for water suppression.<sup>1</sup> Spectra were acquired on a Varian INOVA 500 MHz spectrometer equipped with a triple resonance z-axis gradient probe operating at temperatures ranging from 5 to 35 °C. Data were acquired on a ~0.63-0.75 mM RNA sample (25 mM sodium phosphate, pH 6.8, 100 mM NaCl, 0.1 mM EDTA) in the absence and presence of 1, 5 and 10 molar equivalents for theophylline. 4096 complex points with a sweep width of 12001.1 Hz were collected with 1024 scans per FID and a recycle delay of 2.0 s. Figure S1 shows the theophylline methyl region in the 1D <sup>1</sup>H spectra. As is seen for the RNA imino protons, Figure S1 shows that the theophylline methyl protons do not change chemical shift as a function of the increasing molar ratio of theophylline to RNA, but only change intensities for the free and bound states demonstrating that they are also in slow exchange on the NMR chemical shift time scale.

##### ***1D Lineshape Analysis to Determine the Dissociation Constant for the Theophylline – RNA Complex in the Absence of Mg<sup>2+</sup>***

To determine the K<sub>d</sub> for the theophylline – RNA complex, the lineshapes for the imino resonance of G14 in the free and bound states were simulated using the nlinLS non-linear lineshape analysis and simSpecND simulated spectrum programs contained in the NMRPipe software.<sup>2</sup> The two peaks were first extracted from the full 1D <sup>1</sup>H spectra and used as input in the

nlinLS program along with an initial peak table. The free and bound resonances were simultaneously fit to 1D Lorentzian peak shapes (data not shown).

The apparent  $K_d$  for the theophylline – RNA complex was calculated by determining the fraction RNA bound ( $f_b$ ), which is the intensity of the bound peak divided by the sum of the intensities for the bound and free peaks. An apparent  $K_d$  was then calculated for each titration point (1, 5 and 10 molar equivalents of theophylline to RNA) by fitting to Equation S1

$$f_b = \frac{K_d + [RNA]_{Total} + [Theo]_{Total} - \sqrt{(K_d + [RNA]_{Total} + [Theo]_{Total})^2 - 4[RNA]_{Total}[Theo]_{Total}}}{2[RNA]_{Total}} \quad (S1)$$

in Mathematica 6 (Wolfram Research, Inc.). Table S1 lists the  $f_b$  and calculated  $K_d$  values for each titration point and temperature.  $\Delta H^\circ$  and  $\Delta S^\circ$  values were determined from the  $K_d$  values for temperatures between 5 to 35 °C using the van't Hoff relationship. The linear fit of the data ( $R^2=0.98$ ) yielded  $\Delta H^\circ = -12.1 \text{ kcal mol}^{-1}$  and  $\Delta S^\circ = -0.06 \text{ kcal mol}^{-1} \text{ K}^{-1}$  for the binding reaction. Thus, there is a sizable favorable  $\Delta H^\circ$  and small, unfavorable  $\Delta S^\circ$  for the theophylline-RNA association reaction, consistent with the large number of favorable interactions formed in the complex.<sup>3</sup>

## ***2D Imino <sup>1</sup>H ZZ Exchange Spectroscopy***

2D <sup>1</sup>H ZZ exchange spectra were collected using the pulse sequence shown in Figure S2. Since both <sup>1</sup>H-<sup>1</sup>H ZZ exchange and <sup>1</sup>H-<sup>1</sup>H NOEs give the same sign for cross peaks, a mixing sequence of Markley and co-workers was utilized to eliminate the NOE crosspeaks.<sup>4-6</sup> This sequence relies on the differences in sign and build-up rate for the NOE and ROE crosspeaks.<sup>7</sup> Thus, by setting the NOE mixing time to half that of the ROE mixing time, a pure ZZ exchange spectrum is obtained.<sup>4-6</sup> The ROE mixing time used here consisted of a pair of off-resonance adiabatic sec/tan 180° shaped pulses, with ~4.2 ms pulse widths, centered at ~10 ppm and a ~10.5 ppm bandwidth.<sup>8</sup> The use of off-resonance shaped pulses helps to keep water along the z-

axis. Water magnetization was kept along the +z-axis during  $t_1$  by adding sinc water flip-back shaped pulses before and after the  $t_1$  period.<sup>9</sup> The carrier was shifted to 12.8 ppm during  $t_1$  and then placed back on water for the ZZ mixing sequence<sup>4</sup> and the gradient 11-echo pulses.<sup>1</sup>

2D  $^1\text{H}$  ZZ exchange data were acquired on RNA samples containing 2.6, 3.7, and 6.4 mM total theophylline at 15 °C on a Varian INOVA 600 MHz spectrometer equipped with a cryogenically cooled triple resonance z-axis pulsed-field gradient probe. 2048 and 256 complex points and 14005 and 4700 Hz sweep widths were acquired in the direct and indirect dimensions, respectively. 128 (160 for 2.6 mM theophylline sample) transients were acquired for each FID with an interscan delay of 1.7 s. The following ZZ mixing times were acquired (in random order): 2, 22, 32, 52, 62, 82, 102, 122, 162 for the 2.6 mM theophylline sample; 2 (2x), 15, 27 (2x), 40 (2x), 53 (2x), 65, 78, 103 (2x), 128, 154 and 207 ms for the 3.7 mM theophylline sample; and 2, 19, 36 (2x), 54, 71, 88, 106 (2x), 123, 141, 175, and 210 ms for the 6.4 mM theophylline sample. Several ZZ mixing times were duplicated to estimate experimental errors in the measurements, and no adiabatic sec/tan 180° shaped pulses were used for the shortest mixing time (2 ms). NMR data were processed and analyzed with NMRPipe software.<sup>2</sup>

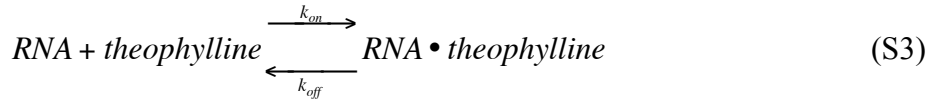
### ***Global Fitting of $^1\text{H}$ ZZ Exchange Spectroscopy Parameters***

A global least-squares fitting procedure, executed in Mathematica 6 (Wolfram Research, Inc.), was used to extract the longitudinal relaxation rates ( $R_1$ ) and the chemical exchange rates ( $k_f$  and  $k_{rev}$ ) from the experimental cross peak intensities. The relaxation and chemical exchange rates were determined by minimizing the difference in experimental and theoretical intensities using the following  $\chi^2$  function,

$$\chi^2 = \frac{\sum_{\tau_m} (f_{\text{mod}}(\tau_m) - f_{\text{data}}(\tau_m))^2}{\Delta f^2} \quad (\text{S2})$$

where  $f_{mod}$  is the function describing the theoretical intensities (see below),  $f_{data}$  is the function describing the experimental data, and  $\Delta f$  is the experimental error. The standard deviation of these rates were estimated from Monte-Carlo simulations<sup>10</sup>; estimates of the experimental errors employed in the simulations were determined from the duplicate measurements at several mixing times. If the errors estimates from the duplicate data were less than 2%, a 2% error was used in the calculations.<sup>10</sup> The Monte Carlo procedure was repeated 150 times for each data set, from which the average rates and standard deviations were determined. The Mathematica 6 notebooks used here are available from the authors upon request.

A two-state model was used to determine rate constants from the 2D <sup>1</sup>H ZZ exchange spectra. For the bimolecular binding reaction of Equation S3, the equations for determining longitudinal relaxation and chemical exchange rates from ZZ exchange data have previously been described<sup>11-13</sup> and are shown below for the diagonal peaks (Equations S4a and S4b) and cross peaks (Equations S5a and S5b).



$$I_{FF}(\tau_m) = I_F(0) \frac{-(\lambda_2 - a_{11})e^{-\lambda_1 \tau_m} + (\lambda_1 - a_{11})e^{-\lambda_2 \tau_m}}{\lambda_1 - \lambda_2} \quad (S4a)$$

$$I_{BB}(\tau_m) = I_B(0) \frac{-(\lambda_2 - a_{22})e^{-\lambda_1 \tau_m} + (\lambda_1 - a_{22})e^{-\lambda_2 \tau_m}}{\lambda_1 - \lambda_2} \quad (S4b)$$

$$I_{FB}(\tau_m) = I_F(0) \frac{a_{21}e^{-\lambda_1 \tau_m} - a_{21}e^{-\lambda_2 \tau_m}}{\lambda_1 - \lambda_2} \quad (S5a)$$

$$I_{BF}(\tau_m) = I_B(0) \frac{a_{12}e^{-\lambda_1 \tau_m} - a_{12}e^{-\lambda_2 \tau_m}}{\lambda_1 - \lambda_2} \quad (S5b)$$

$I_F(0)$  and  $I_B(0)$  are the equilibrium magnetization for the free and bound state, respectively, and  $\tau_m$  is the ZZ mixing time.  $\lambda_{1,2}$  are the eigenvalues of the 2x2 dynamics matrix ( $a_{ij}$ ) describing the loss of magnetization in the free and bound states due to longitudinal relaxation and chemical exchange, given in Equation S6.<sup>11, 12</sup>

$$\lambda_{1,2} = \frac{1}{2} \sqrt{(a_{11} + a_{22}) \pm [(a_{11} - a_{22})^2 + 4k_f k_{rev}]} \quad (\text{S6})$$

where

$$\begin{aligned} a_{11} &= R_{1,B} + k_{rev} \\ a_{12} &= -k_f \\ a_{21} &= -k_{rev} \\ a_{22} &= R_{1,F} + k_f \end{aligned}$$

$R_{1,B}$  and  $R_{1,F}$  are the longitudinal relaxation rates for the bound and free state, respectively.  $R_{1,B}$  and  $R_{1,F}$  are apparent longitudinal relaxation rates and for imino protons represent the sum of the true  $R_1$  and the rate of exchange with solvent.  $k_f$  is the pseudo-first order on rate constant, which equals  $k_{on}[\text{theophylline}]_{Free}$ , and  $k_{rev}$  is  $k_{off}$  (Equation S3).

The data for G4 and G25 were simultaneously fit to the two-state exchange model, where individual  $I_F(0)$ ,  $I_B(0)$ ,  $R_{1,B}$  and  $R_{1,F}$  were determined for G4 and G25 and  $k_{rev}$  and  $k_f$  were fit as a global process. Calculations were performed independently for each theophylline concentration. The exchange cross peaks for G14 were too close to the diagonal to obtain reliable data and were not used in the calculations. Prior to global fitting, the data for G4 and G25 at each theophylline concentration tested were individually fit to the two-state model, which resulted in similar values for  $k_f$  and  $k_{rev}$  in both fits (data not show). Thus, the global fitting procedure was used to further minimize the  $\chi^2$  function. The diagonal and cross peak intensities for G4 and G25 were initially used for fitting Equations S4 and S5; however, this procedure did not accurately reproduce the cross peak data. Specifically, the times of the maximum intensity for the buildup portion of the exchange cross peak curves were not accurately captured (data not shown). Since Equations S4 and S5 depend on all of the kinetic and relaxation rate constants, the cross peak data alone were used in the fitting routine. While fitting to only the cross peak intensities resulted in higher standard deviations for the apparent  $R_1$  relaxation rates, the overall fitting error was lower, and

the experimental cross peak data were more accurately reproduced. The difficulty in fitting the diagonal data likely comes from errors in accurately determining the peak intensities from the overlapped diagonal. The results of the three global Monte Carlo calculations, using the cross peak data alone, are reported in Table S2, and Figure S3 shows the resulting fits to the experimental ZZ exchange data.

## References

- (1) Sklenár, V.; Bax, A., *J Magn Reson* **1987**, 74, 469-479.
- (2) Delaglio, F.; Grzesiek, S.; Vuister, G. W.; Zhu, G.; Pfeifer, J.; Bax, A., *J Biomol NMR* **1995**, 6, 277-293.
- (3) Zimmermann, G. R.; Jenison, R. D.; Wick, C. L.; Simorre, J. P.; Pardi, A., *Nat Struct Biol* **1997**, 4, 644-649.
- (4) Fejzo, J.; Westler, W. M.; Macura, S.; Markley, J. L., *J Am Chem Soc* **1990**, 112, 2574-2577.
- (5) Fejzo, J.; Westler, W. M.; Macura, S.; Markley, J. L., *J Magn Reson* **1991**, 92, 20-29.
- (6) Macura, S.; Westler, W. M.; Markley, J. L., *Methods Enzym* **1994**, 239, 106-144.
- (7) Neuhaus, D.; Williamson, M. P., *The Nuclear Overhauser Effect in Structural and Conformational Analysis*. VCH: New Your, 1989.
- (8) Baum, J.; Tycko, R.; Pines, A., *Phys Rev A* **1985**, 32, 3435-3447.
- (9) Grzesiek, S.; Bax, A., *J Am Chem Soc* **1993**, 115, 12593-12594.
- (10) Choy, W. Y.; Zhou, Z.; Bai, Y. W.; Kay, L. E., *J Am Chem Soc* **2005**, 127, 5066-5072.
- (11) Ernst, R. R.; Bodenhausen, G.; Wokaun, A., *Principles of Nuclear Magnetic Resonance in One and Two Dimensions*. Oxford: Oxford, 1987.
- (12) Farrow, N. A.; Zhang, O. W.; Forman-Kay, J. D.; Kay, L. E., *J Biomol NMR* **1994**, 4, 727-734.
- (13) Palmer, A. G.; Kroenke, C. D.; Loria, J. P., *Methods in Enzymology*, **2001**, 339, 204-238.

**Table S1.** Fraction bound and apparent  $K_d$  for the theophylline – RNA complex in the absence of  $Mg^{2+}$  determined from the peak intensities for the free and bound states of the imino proton of G14.

Temperature (°C)	1 molar equivalents <sup>a</sup>		5 molar equivalents <sup>a</sup>		10 molar equivalents <sup>a</sup>		Average $K_D^c$
	$f_b$	$K_d$ (mM) <sup>b</sup>	$f_b$	$K_d$ (mM) <sup>b</sup>	$f_b$	$K_d$ (mM) <sup>b</sup>	
5	0.44	0.54	0.68	1.4	0.74	2.1	1.3 ± 0.8
10	0.34	1.0	0.60	2.1	0.68	2.8	1.9 ± 0.9
15	0.24	1.8	0.50	3.2	0.59	4.2	3.0 ± 1.1
20	0.13	4.4	0.38	5.3	0.48	6.6	5.4 ± 1.1
25		ND <sup>d</sup>	0.34	6.4	0.45	7.5	6.9 ± 0.8
30	0.10	6.1	0.23	11	0.43	8.1	8.5 ± 2.6
35		ND <sup>d</sup>		ND <sup>d</sup>	0.37	10	10

<sup>a</sup> The concentrations of total RNA and total theophylline were 0.75, 0.69 and 0.63 mM, and 0.75, 3.51 and 6.39 mM, respectively, for the 1, 5 and 10 molar equivalent titration points.

<sup>b</sup> The apparent  $K_d$  calculated using Equation S1.

<sup>c</sup> The average and standard deviation of the apparent  $K_d$  values at a given temperature calculated from all the titration points.

<sup>d</sup> Not determined due to line broadening.

**Table S2.** 2D  $^1\text{H}$  ZZ exchange parameters for imino resonances in the RNA at 15 °C.<sup>a</sup>

	2.6 mM Theophylline		3.7 mM Theophylline		6.4 mM Theophylline	
	G25	G4	G25	G4	G25	G4
$I_{\text{B}}(0) \times 10^6$	$5.9 \pm 0.1$	$11.9 \pm 0.1$	$7.2 \pm 0.1$	$13.3 \pm 0.2$	$22.9 \pm 0.2$	$26.1 \pm 0.3$
$I_{\text{F}}(0) \times 10^6$	$9.0 \pm 0.1$	$15.5 \pm 0.1$	$7.9 \pm 0.1$	$10.7 \pm 0.4$	$9.3 \pm 0.1$	$9.6 \pm 0.1$
$R_{1,\text{B}} (\text{s}^{-1})$	$11 \pm 1.1$	$15 \pm 2.3$	$13 \pm 1.3$	$13 \pm 1.1$	$9.1 \pm 3.6$	$9.2 \pm 3.5$
$R_{1,\text{F}} (\text{s}^{-1})$	$10 \pm 1.2$	$13 \pm 2.3$	$13 \pm 1.3$	$13 \pm 1.1$	$15 \pm 4.8$	$14 \pm 3.4$
$k_{\text{f}} (\text{s}^{-1})$	$0.9 \pm 0.1$		$1.7 \pm 0.1$		$3.1 \pm 0.1$	
$k_{\text{rev}} (\text{s}^{-1})$	$1.7 \pm 0.1$		$1.6 \pm 0.1$		$1.1 \pm 0.1$	
$\chi^2 \times 10^{-4}$	1.6		5.2		10	

<sup>a</sup> Average and standard deviation of ZZ exchange parameters obtained from 150 Monte Carlo calculations performed in Mathematica 6. G25 and G4 were fit to the same exchange rates in a global fit.



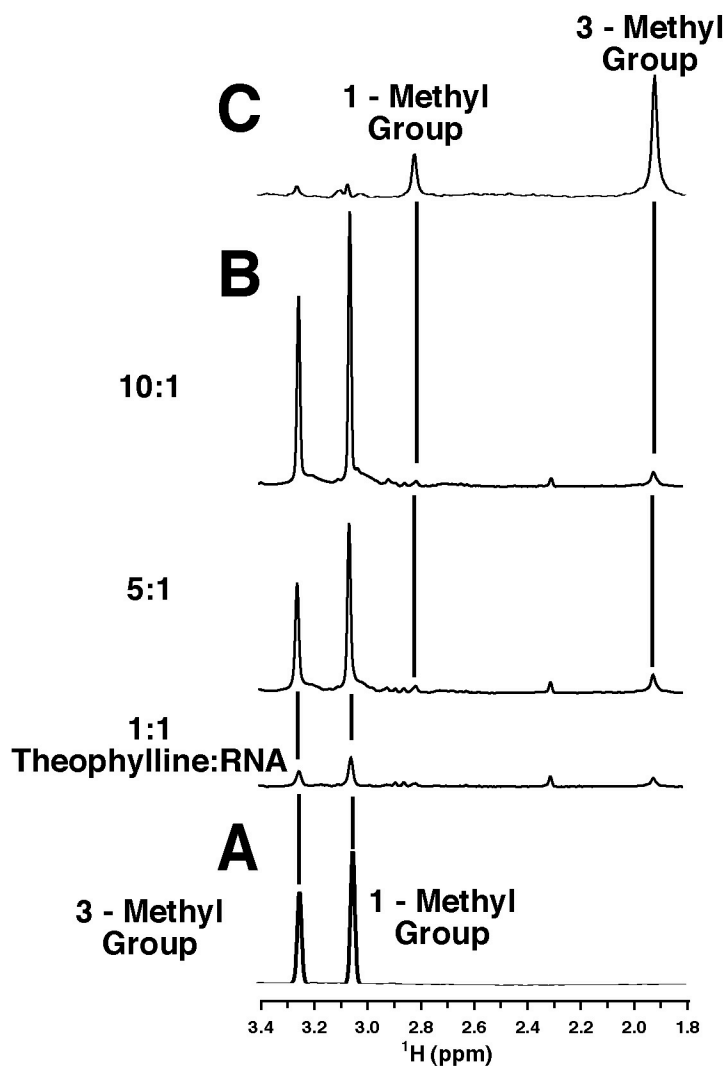


**Figure S1.** Theophylline methyl proton region of the  $^1\text{H}$  1D spectra for the theophylline RNA titration in the absence of  $\text{Mg}^{2+}$  acquired at 500 MHz and 15  $^\circ\text{C}$ . Spectra of the (A) free theophylline showing the assignments of the methyl protons. (B) Titration of RNA with theophylline, showing spectra of the 1:1 ( $[\text{RNA}] = 0.75 \text{ mM}$ ), 5:1 ( $[\text{RNA}] = 0.69 \text{ mM}$ ) and 10:1 ( $[\text{RNA}] = 0.63 \text{ mM}$ ) molar ratio of theophylline:RNA, respectively. (C) The 1:1 complex in the presence of 5 mM  $\text{Mg}^{2+}$  with the methyl proton assignments in the bound state shown.<sup>3</sup> Black lines highlight that the relative intensities and not the positions of the slowly exchanging methyl proton resonances are changing in going from free to bound theophylline.

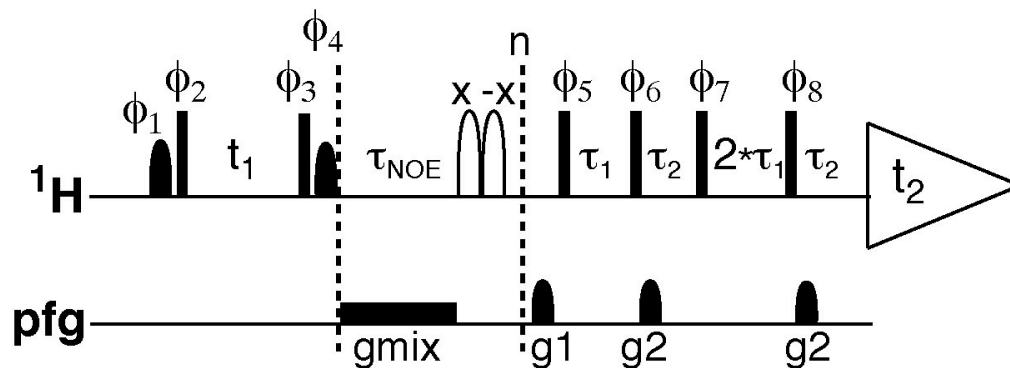


**Figure S2.** Pulse sequence used to measure 2D  $^1\text{H}$  ZZ exchange spectroscopy on the exchanging imino protons. Narrow bars represent  $90^\circ$  pulses, filled shaped are water specific  $90^\circ$  sinc shaped pulses and open shaped are  $180^\circ$  adiabatic sec/tan pulses ( $\sim 4.2$  ms pulse width) that invert the magnetization of resonances downfield of water between  $\sim 5.5$  and 16 ppm. The NOE mixing time,  $\tau_{\text{NOE}}$  is set equal to one-half the length of the ROE mixing time, which occurs during the two  $180^\circ$  adiabatic sec/tan pulses. The delay  $\tau_1$  is  $1/(4 \times \Delta\Omega)$  where  $\Delta\Omega$  is the offset between the imino resonances and water in Hz, and  $\tau_2$  is the time of g2 gradient (2.0 ms) and a  $400 \mu\text{s}$  recovery time. The desired ZZ mixing sequence is obtained by cycling the  $\tau_{\text{NOE}} - 180^\circ(\text{x}) - 180^\circ(-\text{x})$  sequence n number of times. During the NOE mixing time, a low power gradient (0.4 G/cm) is applied, while the gradient strengths for g1 and g2 were 16.6 and 37.3 G/cm, respectively. The phase cycling is  $\phi_1$ : x,-x,x,-x, x,-x,x,-x,  $\phi_2$ : -x,x,-x,x, -x,x,-x,x,  $\phi_3$ : 8(x),  $\phi_4$ : 8(-x),  $\phi_5$ : 4(x), 4(y), 4(-x), 4(-y),  $\phi_6$ : 4(-x), 4(-y), 4(x), 4(y),  $\phi_7$ : x,y,-x,-y,y,-x,-y,x,-x,-y,x,y,-y,x,y,-x,  $\phi_8$ : -x,-y,x,y,-y,x,y,-x,x,y,-x,-y,y,-x,-y,x, and receiver: 4(x), 4(y), 4(-x), 4(-y). Quadrature detection in  $t_1$  is achieved by incrementing the phases of  $\phi_1$ ,  $\phi_2$ , and the receiver according to the States-TPPI protocol.

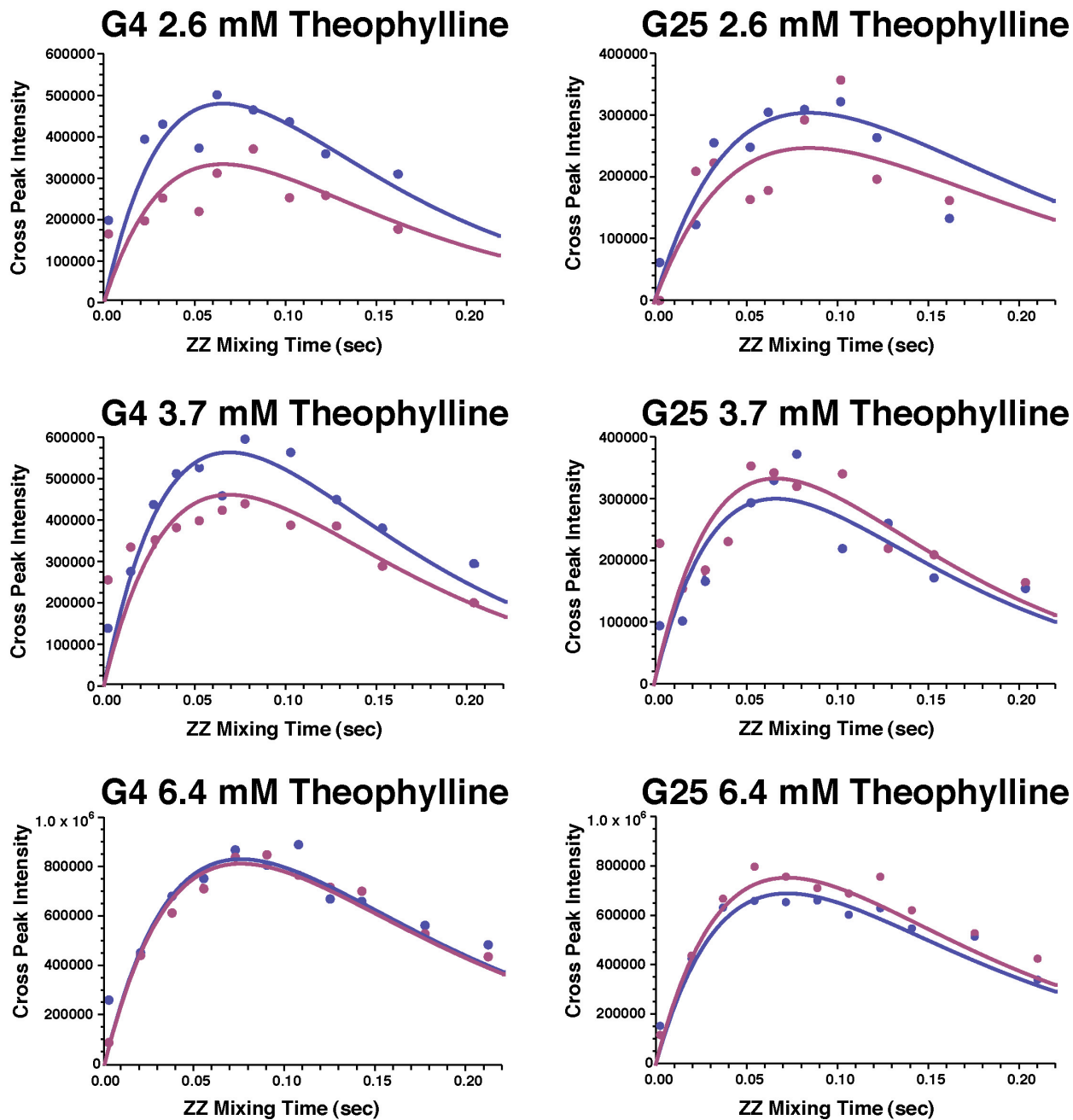


**Figure S3.** Plots of intensity as a function of ZZ mixing time for the exchange cross peaks of the imino proton resonances of G4 (left column) and G25 (right column) in the 2.6, 3.7 and 6.4 mM theophylline samples. Magenta and blue points correspond to the bound-to-free and free-to-bound exchange peaks, respectively. The solid lines in each correspond to the lines of best fit from the global least-squares fit. The data given in Table S2 were used with Equations S5 and S6 to produce each curve.